Chemical Engineering Journal 101 (2004) 23–29

Chemical Engineering Journal

www.elsevier.com/locate/cej

Novel microreactors for functional polymer beads

Takasi Nisisako*, Toru Torii, Toshiro Higuchi

Department of Precision Engineering, Graduate School of Engineering, The University of Tokyo, 7-3-1 Hongo, Bunkyo-ku, Tokyo 113-8656, Japan

Abstract

A novel technique is described for preparing multiple polymeric microspheres of the same size. A monodisperse droplet suspension of an acrylic monomer was prepared in a T-shaped microchannel, and particles of accurately the same size were produced by subsequent polymerization. The droplet/particle size was varied flexibly in the range of diameters 30–120 μm by changing the flow conditions in a microfluidic device. The resulting products have a coefficient of variation (CV) below 2%. A diagram of the flow parameters showed a clear region in which monosized drops were formed successfully. Furthermore, using another microfluidic device, hemispherically colored acrylic microspheres of 90–190 μm in diameter were engineered with a coefficient of variation of less than 1%.

Keywords: Microfluidics; Droplet formation; Bicolored polymeric microspheres; Monodisperse emulsion

1. Introduction

Polymeric microspheres of uniform size in the diameter range 10–100 μm have a great many applications in diverse fields. In liquid chromatography, monosized particles packed optimally in columns provide significant improvement in separation efficiency [1]. Regular-sized beads in liquid crystal displays give a clear and uniform image. Many other applications arise in science and technology including particle-based bioassays [2], flow measurement (such as particle image velocimetry or PIV) and microparticle-based displays [3,4]. As a result there is strong interest in the engineering of polymeric microspheres of the requisite diameter having a tight distribution of sizes.

Classical methods such as emulsion polymerization, mini-emulsion polymerization, and soap-free emulsion polymerization are used to create monodisperse microspheres of less than 1 μm in diameter. Dispersion polymerization can still be used for monosized particles of larger size, but the limit is around 10 μm. Monodisperse particles of diameter larger than 1 μm are better prepared by seed polymerization. In particular, the two-step swelling method of Ugelstad et al. [5] produces monodisperse polymeric particles of diameter greater than 50 μm with a coefficient of variation (CV) of less than 2% [6]. However, this process is rather complicated and require time to obtain final products. Conventionally, polymeric particles of diameter 10–100 μm have been manufactured by suspension polymerization, in which particles are obtained directly by polymerization of the mechanically mixed suspension. Since the droplets in this suspension have a wide size distribution, the resulting particles are generally polydisperse. Tedious and only marginally effective fractionation must then be carried out to realize a tighter size distribution.

Recently, membrane emulsification [7,8] and other techniques [9,10] have proved effective in preparing monodisperse suspensions, and also in the production of monosized polymer beads. Omi et al. [8] successfully manufactured polystyrene microspheres of 2–9 μm with a CV of close to 10% by suspension polymerization of relatively uniform oil/water emulsion produced by sirasu porous glass (SPG) membrane emulsification. Alternatively, microfabricated channel arrays on silicon [9] have been used for preparing suspensions for polymerization and polymeric divinylbenzene beads of over 50 μm with a CV below 5% [10]. These methods still suffer from shortcomings, however. The size of the droplets in suspension depends on the dimensions of the pores/channels so that the size of the resulting particles cannot be changed, and the pore/channel size must be designed smaller than the desired droplet size, so that clogging become a problem in manufacturing smaller microspheres.

Following intensive studies in microfluidic systems, a new approach [11–15] has recently become available for preparing monodisperse droplets. In this technique, two immiscible liquids are introduced into separate microchannels, and then one liquid is forced into the second liquid at a junction to form microdroplets one by one. Droplet formation at

* Corresponding author. Tel.: +81-3-5841-6072; fax: +81-3-5841-6072.
E-mail address: nisisako@intellect.pe.u-tokyo.ac.jp (T. Nisisako).

1385-8947/$ – see front matter © 2003 Elsevier B.V. All rights reserved.
doi:10.1016/j.cej.2003.11.019

the junction is both rapid and reproducible. Furthermore, the resulting droplets are accurately uniform in size, and their size is easily varied by controlling the flow conditions. For example, Thorsen et al. formed water/oil microdrops and several droplet-based patterns such as ribbon and pearl necklace structures in a microfluidic device [11]. We previously studied the rapid and reproducible formation of water/oil microdrops with no surfactant in a hydrophobic microchannel; the maximum breakup frequency (the number of droplets formed per unit of time) was ∼2500 Hz [12–14]. Similarly, monodisperse oil/water microdrops were successfully generated in hydrophilic microdevices [15]. This method overcomes the limitations in other preparation techniques.

We describe below the production of monodisperse polymeric microspheres of diameter 30–120 μm by polymerization of a monomer suspension, which is prepared in a simple T-shaped channel configuration. We also engineer "bicolored" beads using another microfluidic device.

2. Experimental

2.1. Microfluidic devices

All experiments reported here used quartz glass devices. A T-shaped channel was made for generating one-phase monomer droplets, and a sheath-flow channel was made for generating hemispherically colored (bichromal) droplets (Fig. 1). Grooves and holes (supply ports and drain ports, 0.5 mm in diameter) were machined into quartz chips (25 mm × 15 mm, 2 mm thick) using mounted wheels, and by fusion bonding were covered with another quartz chip. As a result of the shape of machine tools, the grooves are rectangular in cross section, unlike isotropically-etched ones. The channels were machined deeper and wider (0.2 mm depth, 0.2–1.0 mm width) near the drain port in order to measure the size of the droplets as spheres there. The channel widens gradually so that the flow speed changes only slowly.

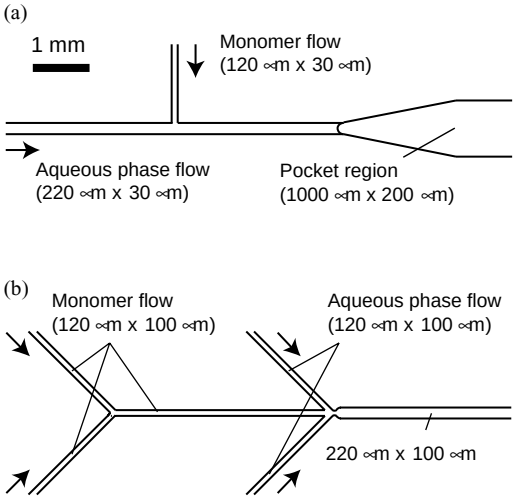

Fig. 1. Schematics of the channel layouts: (a) T-shaped channel, (b) Y-shaped channel and two coflowing channels (channel sizes are written as width × depth). Orientation of flow is specified by arrows.

2.1.1. T-junction device

Fig. 1(a) is a schematic of the T-shaped channel. The organic phase (monomer) flow channel (120 μm wide × 30 μm deep) is at right angles to the aqueous phase flow channel (220 μm wide × 30 μm deep). This T-junction is positioned at 3 mm from the organic phase supply port and 8 mm from the aqueous phase supply port.

2.1.2. Sheath-flow device

The channel configuration for bichromal droplets is shown schematically in Fig. 1(b). There are two main parts: a Y-shaped channel where two-color parallel flow is formed, and a sheath-flow channel where bicolor droplets are generated. The sheath-flow structure is placed 4 mm from the Y-junction and from two supply ports of aqueous phase. The channels for supplying liquids are 120 μm wide × 100 μm deep, and the channel to the pocket region is broader (220 μm wide × 100 μm deep, 4 mm long).

2.2. Materials

1,6-Hexanediol diacrylate (Shin-Nakamura Chemical Co. Ltd., Japan) was used as the organic liquid phase. Polyvinyl alcohol (PVA) aqueous solution (2.0 wt.%) was prepared as the continuous phase liquid. An initiator of photo-induced polymerization (DAROCUR® 1173, Ciba Specialty Chemicals K.K., Japan) was added to the monomer to generate a 1.0 wt.% mixture.

In the preparation of bicolored droplets, isobornyl acrylate (Shin-Nakamura Chemical Co. Ltd., Japan) was chosen as the monomer liquid. For black monomer, carbon black pigment was added to the monomer and a 10.0 wt.% mixture was prepared. For white, titanium dioxide pigments were dispersed in the monomer to give a 10.0 wt.% mixture. An initiator for thermal polymerization was dissolved in both white and black monomers, and 2.0 wt.% mixtures were made. Identical PVA aqueous solution was used in this experiment.

2.3. Equipment and procedures

Glass microsyringes (1000 series, Hamilton Company, NV, USA) were filled with the liquids, and mounted on syringe pumps (KDS200, KD Scientific Inc., PA, USA) which can synchronously operate two syringes at various flow rates. The pumps were tested in advance to confirm constant supply of liquids by using pressure sensors [13]. The glass microchip was assembled in a stainless jig (40 mm × 30 mm × 8 mm) and linked to syringes through polytetrafluoroethylene (PTFE) tubes (0.5 mm i.d. and 1.5 mm o.d.) and connectors.

Table 1
The properties of liquids measured at 293 K

Liquids	Density (g/cm^3)	Viscosity[a] (mPa s)	Surface tension[b] (mN/m)
PVA aqueous solution (2.0 wt.%)	1.00	1.95	44.7
1,6-Hexanediol diacrylate	1.02	6.71	33.5
Isobornyl acrylate	0.99	8.29	29.5

[a] Measured by rotational rheometer.
[b] Measured by bubble-pressure method.

An optical microscope (BX-51, OLYMPUS OPTICAL CO. Ltd., Japan) and a high-speed video camera (Fastcam-max, PHOTRON LIMITED, Japan) were used to observe and record the microfluidic behavior of the two immiscible liquids (so as to capture such phenomena as the formation of microdroplets at junctions). Images were downloaded digitally to an IBM-compatible PC, and the droplet size was calculated from the images.

The resulting droplets were collected in a beaker and cured either by UV light radiation (for 1–2 min) or a hot water bath (70–80 °C for 4–5 min).

To prevent clogging in the microchannels, all equipment was placed in a clean room. The room was air-conditioned to a constant temperature (293 K) to prevent thermally driven fluctuations in the viscosity, surface tension and other physical properties of the fluids (Table 1).

3. Results and discussion

3.1. Preparation of polymeric microspheres with a T-shaped channel

3.1.1. Behavior of two immiscible fluids

Fig. 2 illustrates the variation in flow pattern caused by changes in the continuous phase flow rate (Q_c) at a constant flow rate of the disperse phase (Q_d, 0.1 ml/h). When Q_c was sufficiently low (0.1–0.5 ml/h, i.e., $1 < Q_c/Q_d < 5$), monomer liquid wetted the side wall of microchannel and shaped a stream parallel with the aqueous phase (Fig. 2a); monomer droplets of uniform size were formed regularly (~20 Hz) at the entrance of the pocket (Fig. 2b). Since the difference in speeds of two fluids is relatively small, this effect is driven mainly by the gradient of the interfacial tension at the head of the monomer flow, similar to phenomenon observed in ref. [9]. As Q_c was increased, the point at which drops form started to move upstream (Fig. 2c), and gradually approached the T-junction. At higher Q_c the breakup point finally reached the junction (Fig. 2e), and the droplet size was reduced (Figs. 2e–j), followed by the increase of the breakup frequency; the frequency reached approximately 750 Hz at $Q_c = 18.0$ ml/h. However, when Q_c was increased further, the breakup point moved rapidly downstream, and polydisperse droplets were generated before the pocket area in a disorderly fashion (Fig. 2l). Because of the stabilizer

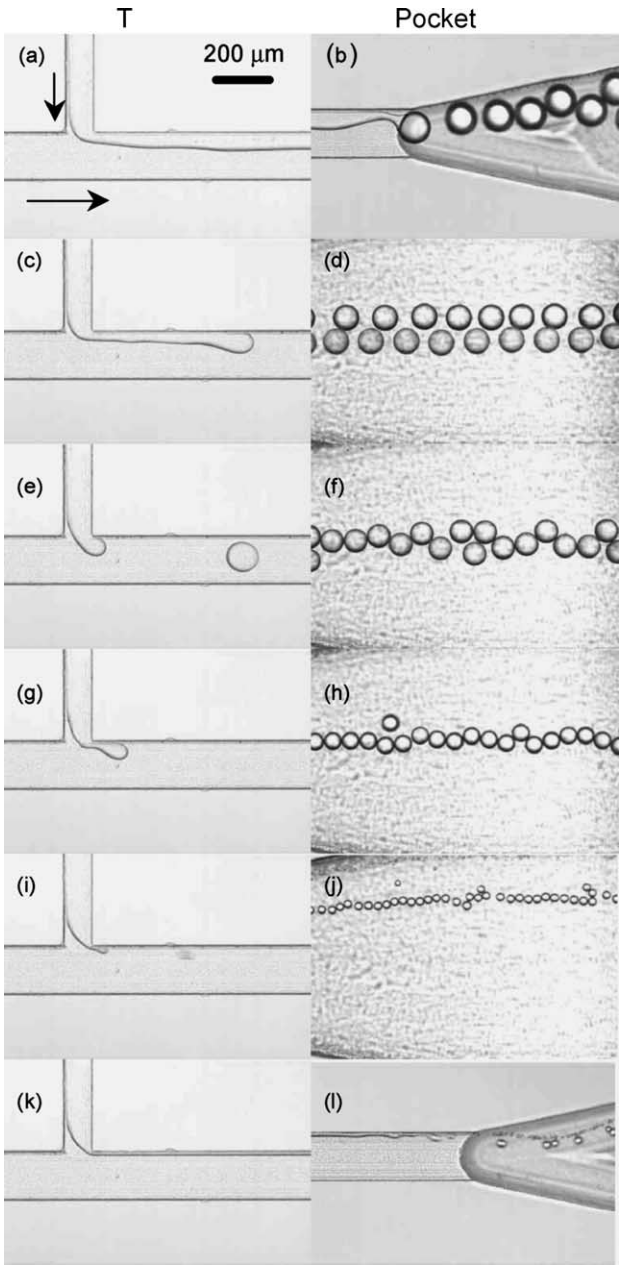

Fig. 2. Patterns of droplet formation observed in the T-junction/pocket when the flow rate of aqueous phase (Q_c) was varied at a fixed monomer flow rate (0.1 ml/h): (a, b) $Q_c = 0.5$ ml/h; (c, d) $Q_c = 1.0$ ml/h; (e, f) $Q_c = 2.0$ ml/h; (g, h) $Q_c = 4.0$ ml/h; (i, j) $Q_c = 18.0$ ml/h; (k, l) $Q_c = 22.0$ ml/h. All these images were recorded at 10 000 fps.

(PVA), no coalescence was observed throughout the flow conditions, even if droplets underwent many contacts with each other in the pocket area.

3.1.2. Effect of flow speed on droplet size

Fig. 3 shows the effect of the aqueous phase flow speed on the diameter of droplets generated at the T-junction. The droplet size decreases as Q_c increases, to reach the limit of drop breakup at the T-junction. Both larger and smaller

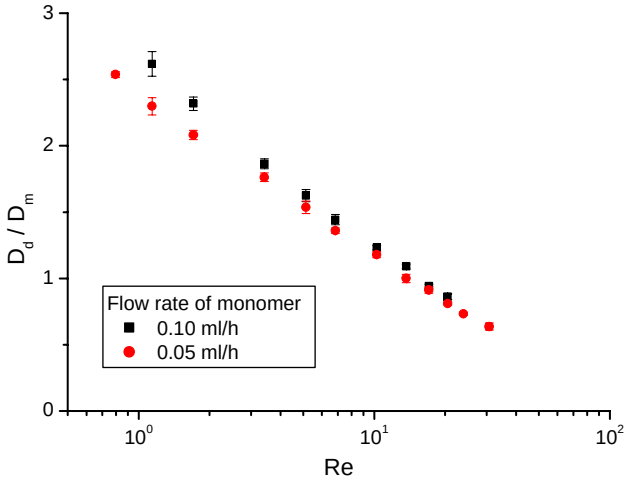

Fig. 3. Effect of aqueous phase flow speed on monomer drop size when droplet breakup is observed at the T-junction. Reynolds number ($\rho v_a D_a \eta_a^{-1}$) on the *X*-axis was calculated with parameters of continuous phase flow (v_a: the average velocity of aqueous phase flow, D_a: equivalent diameter of aqueous flow channel, 52.8 μm). On the *Y*-axis droplet diameter is expressed as a dimensionless number by dividing the measured drop diameter (D_d) by the equivalent diameter of the monomer flow channel (D_m: 48 μm). Error bars on each markers show the standard deviations based on repeated experiments ($n = 5$).

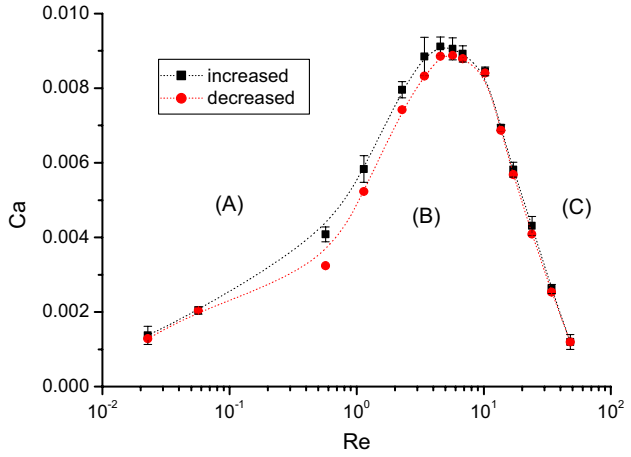

Fig. 4. A flow diagram focusing on droplet breakup at the T-shaped junction. The boundary was studied by varying Q_d by 0.002 ml/h at various values of Q_c. Rectangular markers denote the limits of the droplet formation area measured when Q_d was increased, and circular markers when Q_d was decreased. Error bars indicate the reproducibility of the experiments performed ($n = 10$). Region A: Two immiscible liquids flow together as a continuous stream. (At lower Q_d, droplet formation is observed at the entrance of the deep pocket.) Region B: Monodisperse droplets are formed reproducibly at the T-junction. Region C: Disordered patterns are obtained. At lower Q_d, polydisperse droplets can be observed.

drops than the equivalent diameter of the aqueous phase channel (D_a, 48 μm in this case) were obtained by changing the aqueous phase flow conditions: at $Q_d = 0.1$ ml/h the diameter was 125 μm at $Q_c = 1.0$ ml/h, and 40 μm at $Q_c = 18.0$ ml/h; at $Q_d = 0.05$ ml/h the maximum diameter was 120 μm at $Q_c = 0.7$ ml/h, and 30 μm at $Q_c = 27.0$ ml/h. At lower Q_d, the range of Q_c in which drops were formed was broader. The coefficient of variation was consistently less than 2.0%. The difference in drop diameter observed in the low Reynolds number region gradually decreases with the increase of aqueous phase flow speed. This suggests that Q_d is significant in determining the droplet size in the low Reynolds number region ($Re \sim 10^0$) but that its influence on droplet size declines at higher Reynolds numbers ($Re \sim 10^1$). This also implies that, in the higher *Re* region, the variation of Q_d determines the breakup frequency rather than the droplet size.

3.1.3. The flow diagram focusing on droplet formation

Fig. 4 shows the flow diagram obtained in our experiments. The vertical axis is the capillary number, given by

$$\mathrm{Ca} = \frac{\eta v}{\gamma} \quad (1)$$

where Ca is the capillary number, η the monomer viscosity, v the average velocity of the monomer, and γ the interfacial tension between the two fluids. We used the values $\eta = 6.71$ mPa s, $\gamma = 11.2$ mN/m in our calculations. Marks on the graph show the boundary between the droplet formation area and other regions. Those points were obtained by varying Q_d at various values of Q_c.

At low Q_c ($Re < 10^0$), the limit of Q_d below which droplets are formed is also low; above the boundary, the monomer flow and the aqueous phase form parallel streams flowing into the pocket area, and droplets form there spontaneously as shown in Fig. 2b (Region A). As *Re* increases in the system, the limit of Q_d also increases. Then, above a certain *Re* (~4), the limit of Q_d starts to decrease, and becomes less than 1/9 of the maximized limit of Q_d (~0.2 ml/h) at $Re \sim 10^2$; beyond the boundary, disordered breakup of droplets is observed along the channel wall (Region C).

There are several important points. First, drop breakup at a T-junction is observed in a limited area in the flow diagram (Region B), which is surrounded by the low *Re* area (Region A) and the disordered pattern area (Region C). Within this limited area, the droplet size and breakup frequency are controllable. Second, this area shows a peak where Q_d is maximized. This means that the greatest productivity can be achieved at definite conditions of the aqueous phase. Although more work is needed with various channel configurations and pairs of liquids, this is already valuable information for evaluating the productivity of microfluidic devices. Finally, sufficiently small capillary number ($\mathrm{Ca} < 10^{-2}$) in Region B indicates that interfacial tension effects dominate the droplet formation in this system.

3.1.4. Polymerized beads

In Fig. 5 we show a sample of microspheres prepared by subsequent polymerization. Monosized particles were obtained in the range of 30–120 μm in diameter with a CV of 1–2%.

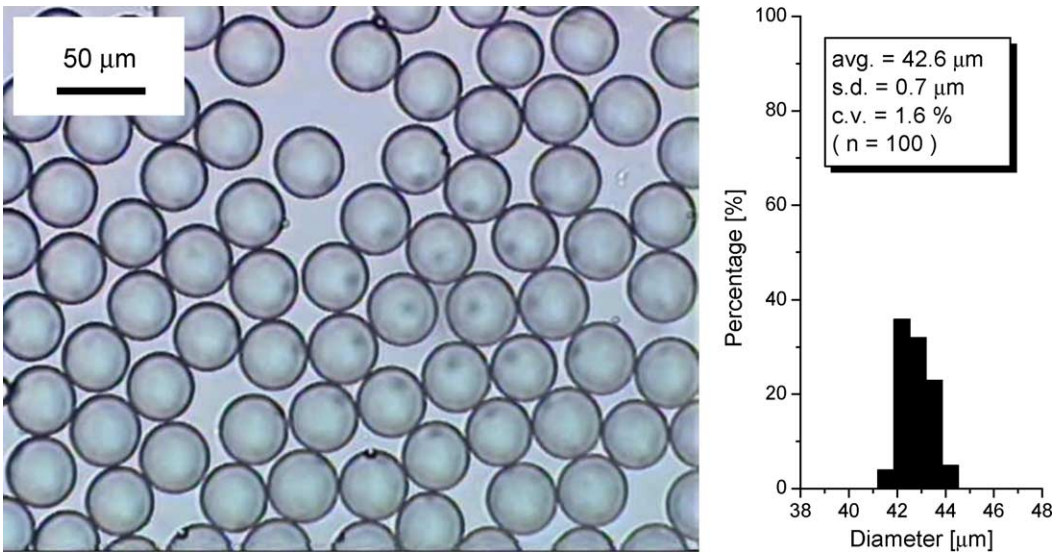

Fig. 5. Left: monodisperse microspheres (poly(1,6-hexanediol diacrylate)) cured by photo-induced polymerization. Right: size distribution of beads prepared (mean diameter = 43 μm, CV = 1.6%).

Although they are hardly visible in the pictures in Fig. 2, the formation of "satellite" droplets (diameter <5 μm) was observed in the breakup process of "primary" droplets. Throughout the flow conditions within Region B (Fig. 4), one or several satellite drops are formed when a primary droplet is formed at the T-junction, even when the aqueous flow speed is very low (e.g., $Re < 10^{-1}$). Strictly, then, droplets formed at the T-junction are "bi-disperse" or "tri-disperse", and not monodisperse. However, the size distribution of the primary drops is very narrow because of the periodical and reproducible generation of satellite droplets. They can easily be removed by conventional filtration techniques, although consumption of material would be a problem in the production of particles of smaller size.

The present quantity of product is only on the laboratory scale, and the improvement of productivity will be strongly demanded for the commercialization on the industrial scale. The concept of numbering-up [16] of the same microdevices can be applied for that purpose, but nevertheless the improvement of productivity per single unit is essential. One possible idea for multiplying the output on a chip is to supply one liquid as a stream and then divide it into a number of microstreams. In this case, careful consideration of channel geometry will be vital because flow rates in multiple channels have to be distributed equally for preparing highly monodisperse droplet suspension as droplet size is sensitive to flow conditions in our method as mentioned above.

3.2. Formation of bichromal droplets in a sheath-flow device

Using the sheath-flow device shown in Fig. 1b, we successfully prepared bicolored droplets.

3.2.1. Formation of two-color flow at a Y-junction

Two differently colored monomers were driven into the channels through two separate inlets. When they were driven at the same flow rate, the two monomers came together and formed a two-colored parallel flow at the Y-junction in which the color boundary was clearly visible, and the flows of both colors were of approximately equal width. When the flow rates of the monomers were in the range 0.1–1.0 ml/h, the Reynolds number in this stream was extremely small ($Re < 10^{0}$). The flow was therefore laminar, and no color mixing by turbulence was observed at the point of confluence. Also, two-colored flow reached the sheath-flow junction without blurring of the color boundary in this range of flow rates. Mixing in laminar conditions is well known to be dominated by diffusion, but the residence time of bicolored flow in the channel (4.0 mm long) was calculated to be less than 1.0 s in our experiments, short enough to preclude color mixture by diffusion.

3.2.2. Droplet formation at a sheath-flow junction

Fig. 6 shows the process of breakup of bicolored droplets at a sheath-flow point. The two-color flow reaches the sheath-flow junction, and bicolored droplets were formed from the symmetrically coflowing aqueous liquids. These droplets were produced at constant frequency and were of uniform size. When the coflowing aqueous streams were sufficiently closely balanced in speed, the droplets generated had clear color edges, but when the speeds of the two aqueous streams differed considerably, convection occurred in monomer ligaments and color mixing was observed. The correct choice of speeds of the liquids is therefore essential to precise determination of the color distribution.

This sheath-flow structure was also applicable to the preparation of single-phase droplets. Monodisperse

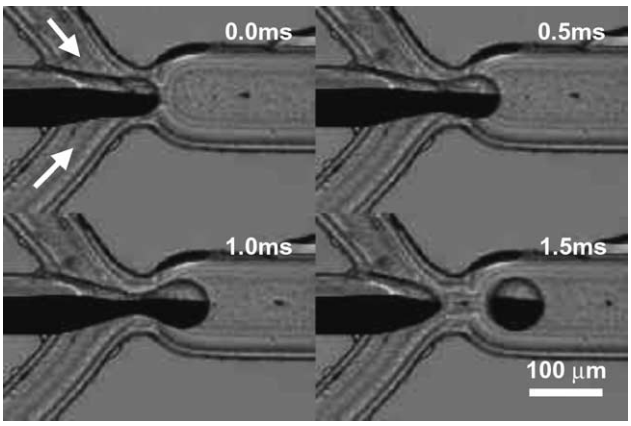

Fig. 6. Formation of a bicolored droplet at the sheath-flow junction. To capture clear images of the color edge, white pigments were not used in this case; black/transparent droplets were prepared in these images. Frames were captured at 2000 fps by a high-speed video camera.

monomer drops were produced like in the case of T-junction device.

3.2.3. Continuous phase flow speed versus droplet size

In this symmetrical coflowing system, the droplet size was dependent on the flow speed of the aqueous phase, as shown in Fig. 7. When the speed of the two-color monomers and the two coflowing aqueous streams were balanced in both pairs, the droplet size could be varied widely without losing the distinct color border. Fig. 7 shows the relation between the aqueous phase flow rate and the size of the droplets generated. At each flow condition marked on the graph, the droplets were bicolored and uniform in size (CV < 1.0%); see Fig. 8. The droplet size decreases as the aqueous phase flow speed increases, although a limit is reached, as in the case of a T-shaped channel. The maximum diameter observed was approximately 190 μm while the minimum was about 90 μm.

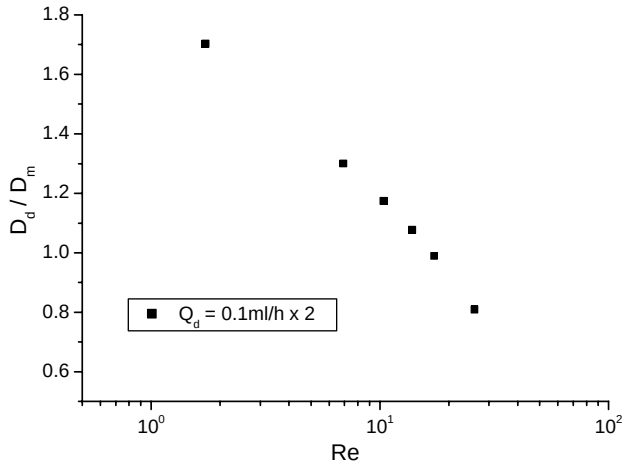

Fig. 7. Effect of aqueous phase flow speed on bicolored droplet size. $D_m = 109\,\mu m$.

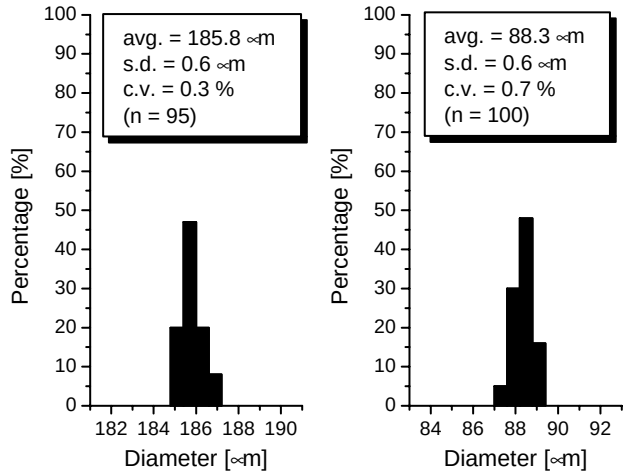

Fig. 8. Size distribution of bicolored droplets prepared for differing flow rates of Q_c (left: $Q_c = 2.0$ ml/h, right: $Q_c = 30.0$ mlh).

3.2.4. Preparation of bichromal beads by curing

Fig. 9 shows bichromal beads that have been cured by heat-induced polymerization. A less distinct color border was noticed in some spheres. Also, some spheres with distinct color boundaries were not colored hemispherically. These effects are believed to be due to the drain path, to the pocket region in the chip, to holes in the jig, and to space in the tube. Both convection and diffusion are believed to reduce the quality of the balls. One promising way to tackle the problem is to reduce the dead volume in the drain route. The subsequent polymerization process may also act to reduce the waiting time for droplets to be cured and prevent diffusion mixing.

With further refinement (such as control of electric charge on both hemispheres), these products may be used in twisting-ball displays [3]. Though the present report concentrates on colored balls, we believe that this strategy is applicable to many other materials to create polymeric beads with a specified combination of materials, properties and sizes.

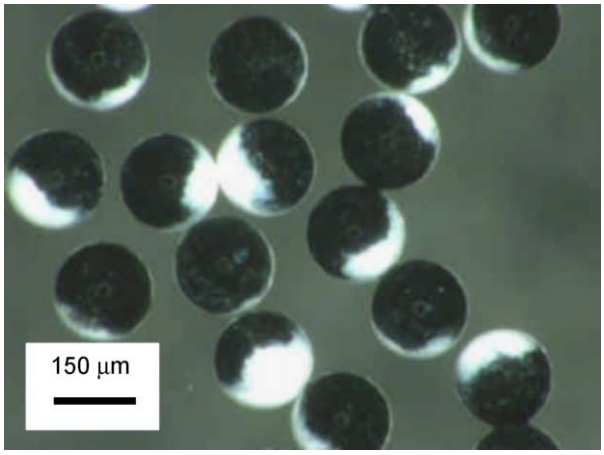

Fig. 9. Polymerized bicolored beads.

4. Conclusions

We have reported here the production of polymeric microspheres using confluent microflow systems. Monomer droplets of uniform size were rapidly and reproducibly formed in the crossflow junction, and polymer particles with a CV below 2% were successfully prepared by subsequent polymerization. The particle size was reliably chosen in the range of 30–120 μm by controlling flow conditions. A flow diagram focusing on droplet breakup phenomena was obtained. This simple technique will be applicable to a variety of functional spheres: porous particles, magnetized beads, microcapsules, and many others.

We showed a further functionality by preparing hemispherically colored droplets and microspheres that were cured subsequently. These functional particles could find application as materials in electric displays, as Gyricon balls have done [3]. The possibility of active control of the internal design of particles now arises. This method shows great promise and we believe that it will open up a new field of research in the microfluidic synthesis of pioneering materials.

Acknowledgements

This work was supported partly by grants from the Research Association of Micro Chemical Process Technology (MCPT) of Japan, Grant-in-aid for Scientific Research from MEXT (No. 15310100), Special Coordination Funds for Promoting Science and Technology. The authors would like to thank the cooperation of Takanori Takahashi and Yoichi Takizawa (Soken Chemical & Engineering Co. Ltd.) in the preparation of bicolored droplets/spheres.

References

[1] J. Ugelstad, L. Søderberg, A. Berge, J. Bergstrøm, Nature 303 (1983) 95.
[2] J.P. Nolan, L.A. Sklar, Trends Biotechnol. 20 (2002) 9.
[3] N.K. Sheridon, M.A. Berkovitz, SID Int. Symp. Dig. Tec. (1977) 114.
[4] B. Comiskey, J.D. Albert, H. Yoshizawa, J. Jacobson, Nature 394 (1998) 253.
[5] J. Ugelstad, et al., Makromol. Chem. 180 (1979) 737.
[6] J. Ugelstad, et al., J. Polym. Sci. 72 (1985) 225.
[7] T. Nakashima, M. Shimizu, M. Kukizaki, Adv. Drug Deliv. Rev. 45 (2000) 47.
[8] S. Omi, K. Katami, A. Yamamoto, M. Iso, J. Appl. Polym. Sci. 51 (1994) 1.
[9] S. Sugiura, M. Nakajima, S. Iwamoto, M. Seki, Langmuir 17 (2001) 5562.
[10] S. Sugiura, M. Nakajima, M. Seki, Ind. Eng. Chem. Res. 41 (2002) 4043.
[11] T. Thorsen, R. Roberts, F. Arnold, S. Quake, Phys. Rev. Lett. 86 (2001) 4163.
[12] T. Nisisako, T. Torii, T. Higuchi, in: Proceedings of the Micro Total Analysis Systems 2001, Monterey, CA, USA, 2001, p. 137.
[13] T. Nisisako, T. Torii, T. Higuchi, Lab. Chip 2 (2002) 24.
[14] T. Nisisako, T. Torii, T. Higuchi, in: Proceedings of the 6th International Conference Microreaction Technology (IMRET6), New Orleans, LA, USA, 2002, p. 415.
[15] T. Nisisako, T. Torii, T. Higuchi, in: Proceedings of the 16th International Conference Microelectromechanical systems (MEMS-03), Kyoto, Japan, 2003, p. 331.
[16] W. Ehrfeld, V. Hessel, H. Lowe, Microreactors, Wiley–VCH, 2000.